

Electronic Supporting Information

Investigating the thermal stability of ultra-small Ag, Au and AuAg alloy nanoparticles embedded in silica matrix

Hemant Jatav¹, Maja Mičetić², Anusmita Chakravorty¹, Ambuj Mishra¹, Matthias Schwartzkopf³, Andrei Chumakov³, Stephan V. Roth^{3,4} and Debdulal Kabiraj^{1*} (✉)

¹Materials science department, Inter-University Accelerator Centre, Aruna Asaf Ali Marg, New Delhi, 110067, India

²Ruđer Bošković Institute, Bijenička cesta 54, Zagreb 10000, Croatia

³Deutsches Elektronen-Synchrotron (DESY), Notkestraße 85, D-22607 Hamburg, Germany

⁴KTH Royal Institute of Technology, Department of Fibre and Polymer Technology, Teknikringen 56-58, SE-100 44 Stockholm, Sweden

Corresponding Author*: Dr. Debdulal Kabiraj (d.kabiraj@gmail.com)

Content:

Page 3: **Figure S1** RBS spectra of (a) Au/SiO₂ and (b) Au-Ag/SiO₂ NC thin film.

Page 3: **Figure S2** Raw GISAXS data of Au-Ag/SiO₂ NC after different annealing temperatures.

Page 4: **Figure S3** Evolution in the NP size distribution estimated using GISAXS analysis.

Page 5: **Figure S4** GIWAXS analysis of (a) Au-Ag/SiO₂ and (b) Au-Ag/SiO₂ at room temperature and 800°C.

Page 5: **Table. S1.** Parameters of the simulated GISAXS maps for Au-Ag/SiO₂.

Page 5: **Table. S2.** Parameters of the simulated GISAXS maps for Au/SiO₂.

Page 6: **Figure S5.** (a) HAADF-STEM images and (b) Scanning TEM energy-dispersive X-ray spectroscopy elemental mapping of AuAg nanoparticles (NPs) inside silica matrix at 900 °C.

Page 7: **Figure S6.** (a) HAADF-STEM images and (b) Scanning TEM energy-dispersive X-ray spectroscopy elemental mapping of Au nanoparticles (NPs) inside silica matrix at 900 °C.

Page 8: **Figure S7.** HRTEM image of AuAg-SiO₂ NC after annealing at different temperatures.

Page 9: **Figure S8.** HRTEM image of Au-SiO₂ NC after annealing at 400°C.

Page 9: **Figure S9.** HRTEM image of Ag-SiO₂ NC after annealing at 400°C.

Page 10: **Figure S10.** The core-level XPS spectra of the Ag and Au components of Ag, Au and Au-Ag NCs.

Page 11: **Figure S11.** Optical absorbance of as-deposited (red) and 800 °C annealed (black) silica thin-film (without metal) deposited on quartz substrate.

Synthesis: The nanocomposite (NC) thin films consisting of metal nanoparticles (NPs) inside the silica matrix were prepared using Atom Beam Sputtering (ABS) technique. The detailed information about the setup and operating conditions are reported in our previous paper [1]. The composition of the elements was controlled by the sputtering rate and the relative area exposed to the 600 eV neutral Argon atom beam. For AuAg/SiO₂ NCs, four foils of Au and Ag each, with an optimized surface area were pasted to a quartz target (3 inch diameter), and then all three components (Metal, Si, and O) were co-sputtered under high vacuum in an ABS chamber to prepare the desired thin-films on the Si and quartz substrate. The surface area of each metal foil used for deposition was 5 × 5 mm². Due to its optical transparency, quartz substrate was selected for UV-Visible absorption spectroscopy measurements, while silicon substrate was used for all other characterizations. Similarly, for Au/SiO₂ and Ag/SiO₂NCs, four metallic foils of Au and Ag respectively were pasted over quartz target. The surface area of each metal foil was kept same.

Rutherford Backscattering spectrometry (RBS): RBS measurement was performed to evaluate the film thickness and relative metal concentration of (a) Au/SiO₂ and (b) AuAg/SiO₂ NC. The film thickness of (260 ± 18) nm and (270 ± 19) nm is observed for Au/SiO₂ and Au-Ag/SiO₂ NC respectively.

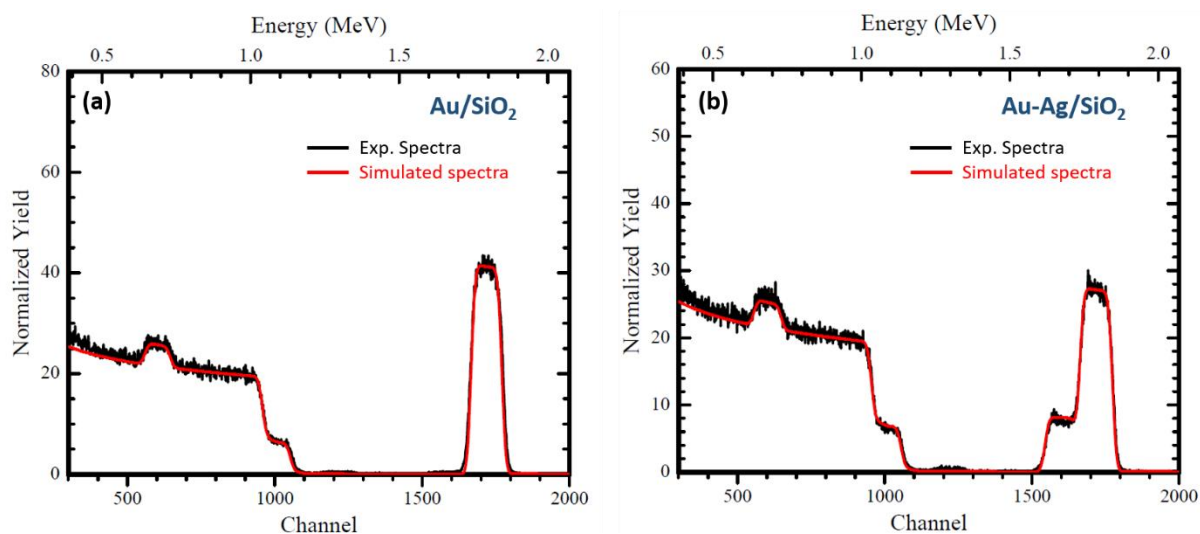


Figure S1 RBS spectra of (a) Au/SiO₂ and (b) Au-Ag/SiO₂ NC thin film. Here red solid line shows the fitted spectra simulated using Rutherford Universal Manipulation Program (RUMP) [2].

Grazing-incidence small/wide-angle X-ray scattering:

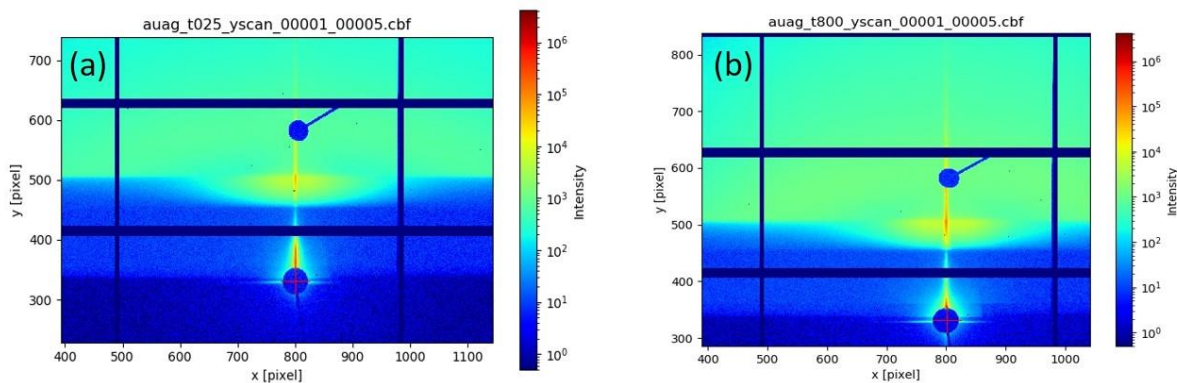


Figure S2 Raw GISAXS data for AuAg/SiO₂ nanocomposite after annealing at (a) 25 °C and (b) 800 °C. The gap lines in the intensity distribution is removed in the manuscript to compare them with simulated spectra.

The form factor and structure factor are the two key contributors to a 2D GISAXS intensity distribution map. The shape factor is basically a Fourier transformation of NPs' shape and can be determined by the *a priori* information of spherical NPs' shape from HRTEM images. However, determining the ordering of NPs (also known as the structural factor) is challenging and requires careful consideration. In our analysis, we utilized 3D-paracrystalline model [3, 4]

to define NPs positioning and structure factor. As a result, information about the NPs' separations in lateral (a) and vertical (c) directions and also the NP radius in lateral (R_L) and vertical (R_V) directions are calculated. Here, σ_R indicates the standard deviation in calculated radius. Even for the highest annealing temperature (AT), only one mean size distribution is considered (no bimodal size distribution). The results estimated from GISAXS analysis are listed in Table. S1 and S2.

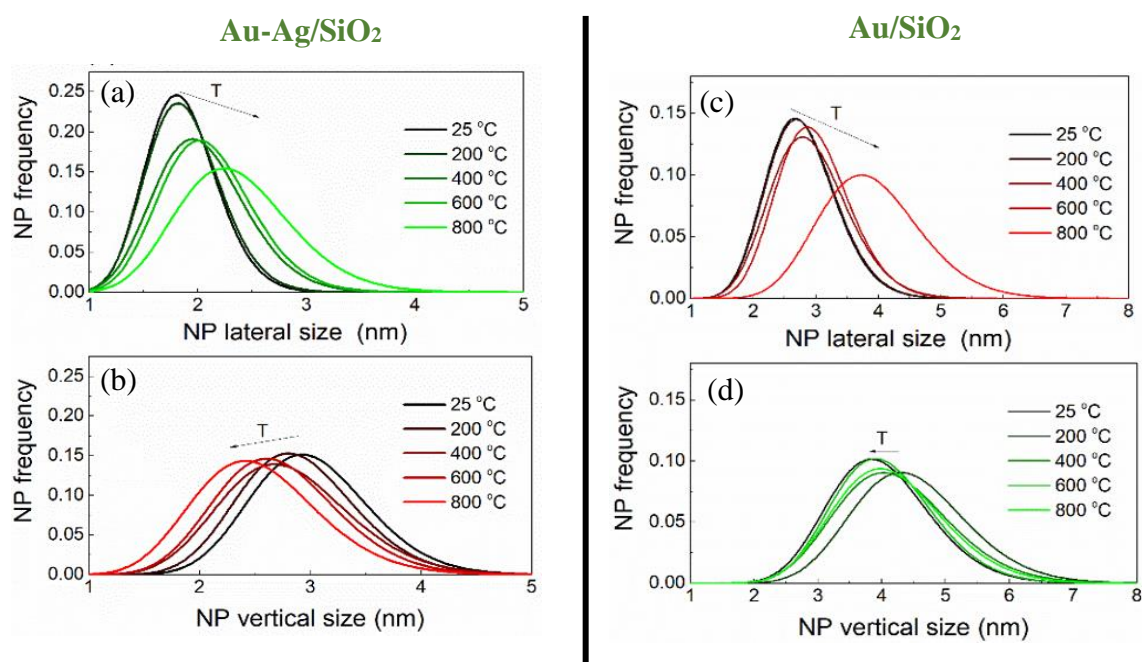


Figure S3 Evolution in the NP size distribution (unimodal) is plotted with respect to AT in (a) lateral and (b) vertical directions for Au-Ag/SiO₂ NC. Mean NP size is increasing with rise in AT in lateral direction (S3 a). However, it is decreasing in vertical direction (S3 b). Similar graphs are plotted for Au/SiO₂ NC in (c) and (d). For Au-Ag/SiO₂ NC, a sudden change in NP mean size is observed at 800 °C.

In Figure S4, one-dimensional GIWAXS intensity spectra for (a) Au-Ag/SiO₂ (RT) and (b) Au-Ag/SiO₂ (800 °C) are fitted with Lorentzian and Voigt function after the linear background corrections to evaluate the peak positions and width. Similar calculations were also done for (d) Au/SiO₂ (RT) and (e) Au/SiO₂ (800 °C). The change in the minimum NP size of the metal NPs is estimated using GIWAXS analysis (Debye-Scherrer formula) at different annealing temperatures [5]. The estimated minimum crystallite size for Au-Ag/SiO₂ varies from 2.20 nm to 2.16 nm, with rise in temperature from RT to 800 °C. For Au/SiO₂, the minimum crystallite size varies from 2.74 nm to 3.85 nm, with rise in temperature from RT to 800 °C.

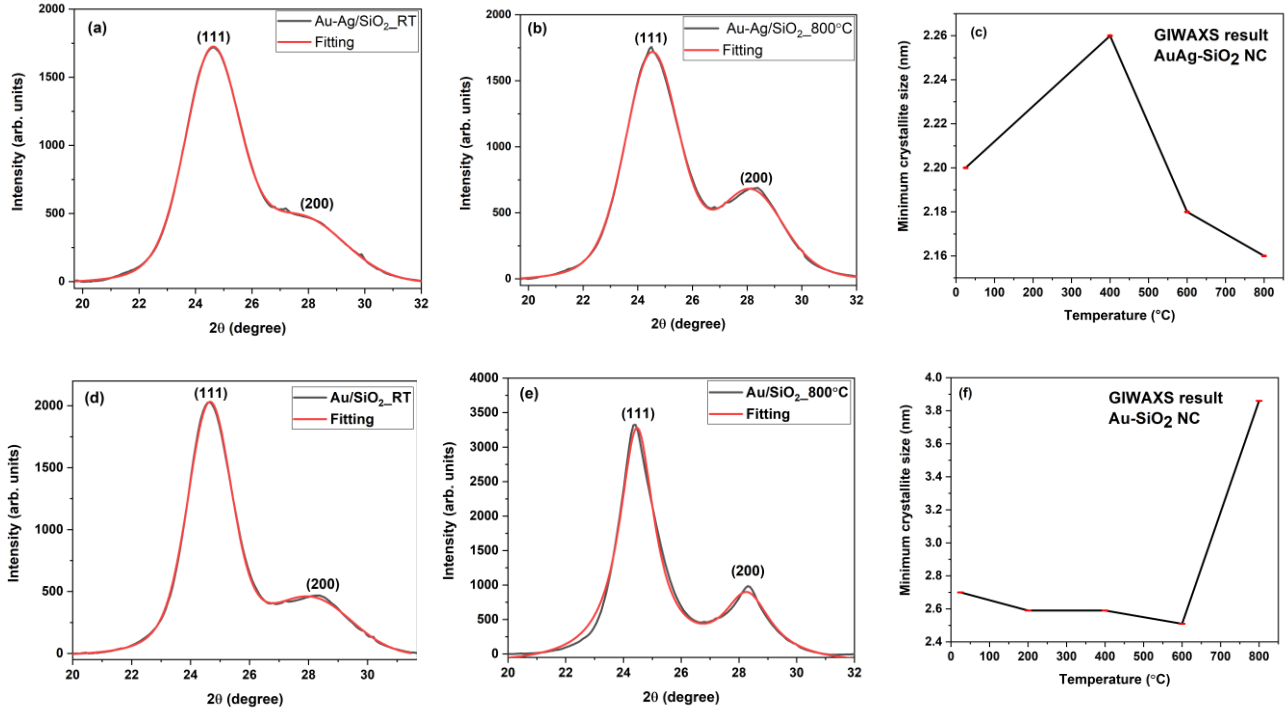


Figure S4. 1-dimensional GIWAXS intensity spectra for (a) Au-Ag/SiO₂ (RT) and (b) Au-Ag/SiO₂ (800 °C). (c) Plot for minimum crystallite size with increase in annealing temperature. Similarly, spectra are fitted for (d) Au /SiO₂ (RT) and (e) Au /SiO₂ (800 °C). The calculated minimum crystallite size with increase in annealing temperature is plotted in (f). Error bars are merged in the data points.

Table S1. Parameters of the simulated GISAXS maps of AuAg/SiO₂. All values are given in nm. Here NPs' separations in lateral and vertical directions are denoted by a and c . σ_R indicates the standard deviation in calculated radius. R_L and R_V are the NPs' radius in lateral and vertical directions.

Sample	a	c	$\sigma_{1(x,y)}$	$\sigma_{1(z)}$	$\sigma_{3(x,y)}$	$\sigma_{3(z)}$	R_L	R_V	σ_R
RT	4.1	6.0	1.3	3.6	2.0	1.8	0.9	1.5	0.3
200 °C	4.1	5.9	1.4	4.0	2.2	1.8	0.9	1.4	0.3
400 °C	4.1	6.0	1.1	4.8	2.1	2.1	1.0	1.4	0.3
600 °C	4.1	6.0	1.2	4.7	2.1	2.1	1.0	1.4	0.3
800 °C	4.1	5.9	1.3	4.5	2.2	2.1	1.2	1.3	0.3

Table S2. Parameters of the simulated GISAXS maps of Au/SiO₂. All values are given in nm.

Sample	a	c	$\sigma_{1(x,y)}$	$\sigma_{1(z)}$	$\sigma_{3(x,y)}$	$\sigma_{3(z)}$	R_L	R_V	σ_R
RT	3.9	8.2	3.0	4.7	3.4	2.3	1.4	2.2	0.3
200 °C	4.0	8.0	3.0	5.7	3.8	2.3	1.4	2.2	0.3
400 °C	4.0	7.8	3.4	6.9	3.6	2.4	1.5	2.1	0.3
600 °C	3.9	7.8	3.4	6.9	3.6	2.4	1.5	2.1	0.3
800 °C	4.2	7.5	5.8	11.2	5.2	3.9	2.0	2.1	0.4

Transmission Electron Microscopy:

(i) HAADF-STEM imaging and EDS elemental mapping

High-angle annular dark-field imaging (HAADF) were acquired in STEM mode for Au-Ag NPs inside silica matrix at 900 °C (FIG. S5). It can be seen that silicon and oxygen are uniformly distributed throughout the nanocomposite thin film, whereas Silver and gold are uniformly distributed inside the NPs, confirming the formation of alloy NP. The most of the NPs are observed spherical in shape. Similar, HAADF-STEM images of Au NPs inside silica matrix at 900 °C are shown in FIG. S6. The presence of Au atoms inside the NPs are confirmed by EDS elemental mapping. Previously in our paper, elemental mapping of Ag NPs inside the silica matrix was shown [1].

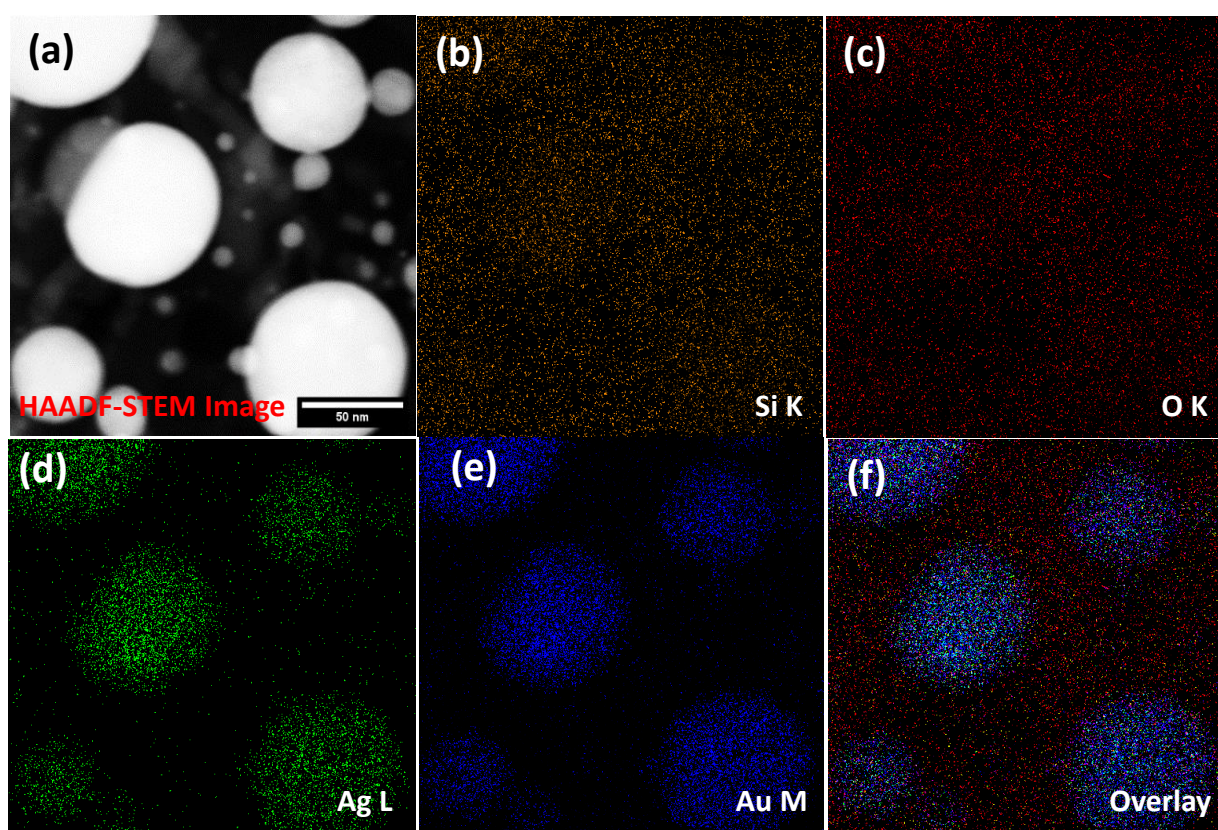


Figure S5 . (a) HAADF-STEM image of Au-Ag NPs inside silica matrix after annealing at 900 °C. Scanning TEM energy-dispersive X-ray spectroscopy elemental mapping of (b) Silicon-K (c) Oxygen-K and (d) Silver-L (e) Gold-M edge. (f) Overlay of b, c, d and e images. The bar scale of all the images are same as shown in image (a), i.e. 50 nm. Here, Ag and Au presence is shown by green and blue colors respectively.

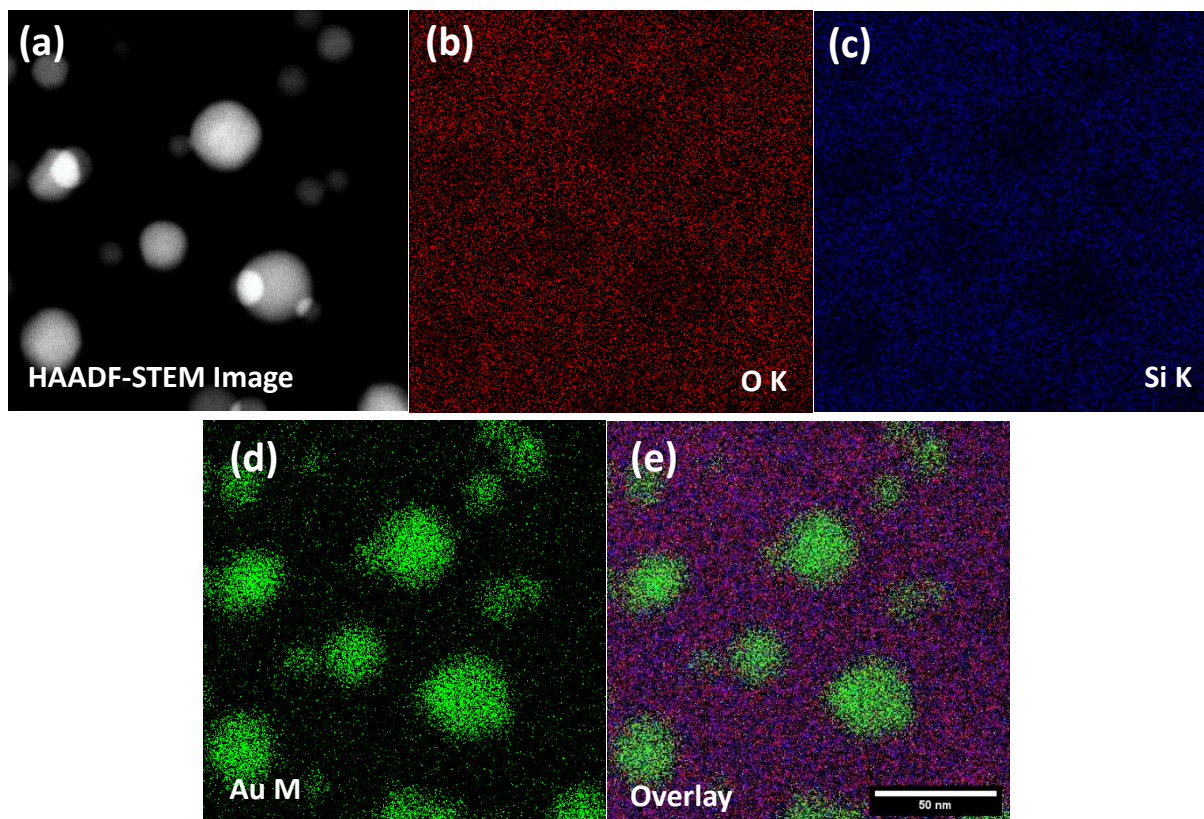
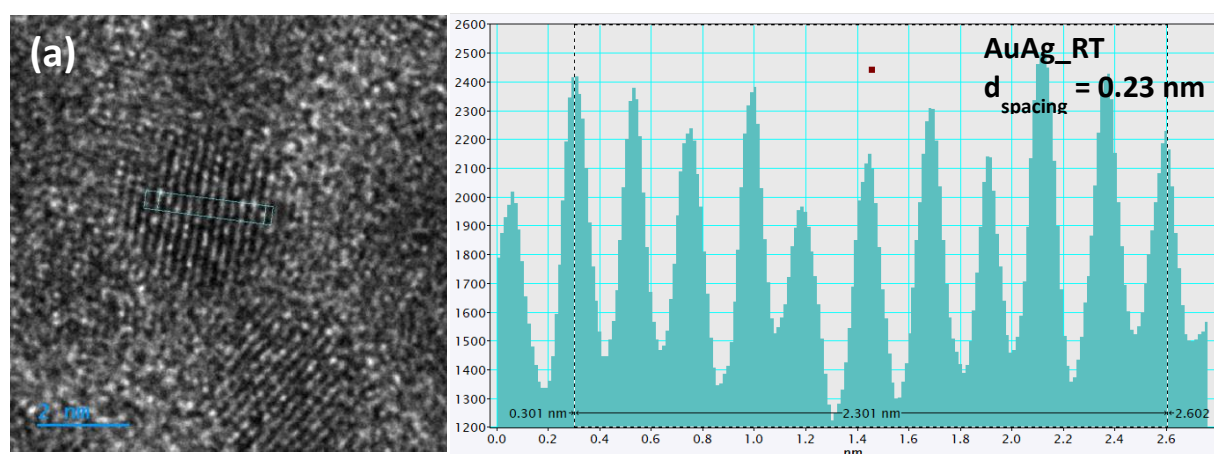


Figure S6. (a) HAADF-STEM images of Au NPs inside silica matrix at 900 °C. Scanning TEM energy-dispersive X-ray spectroscopy elemental mapping of (b) Oxygen-K (c) Silicon-K and (d) Gold-M edge. (e) Overlay of b, c and d images. The bar scale of all the images are same as shown in image (e), i.e. 50 nm.

(ii) High resolution TEM images: HRTEM images were acquired after annealing at different temperatures to evaluate the thermal stability of lattice fringes of Au-Ag/SiO₂. It can be seen for as-deposited sample that majority of the NPs are having single domain crystal structure (i.e. all the lattice fringes are aligned in one particular orientation) and d spacing is calculated as ~0.23 nm. Interestingly, the d spacing remains unchanged and single domain structure is sustained over the entire range of annealing temperature, upto 900 °C. These results show the structural stability of embedded NPs upon thermal annealing upto 800 °C. Similar, single domain crystal structure is also been observed for Au/SiO₂, and Ag/SiO₂ NCs.



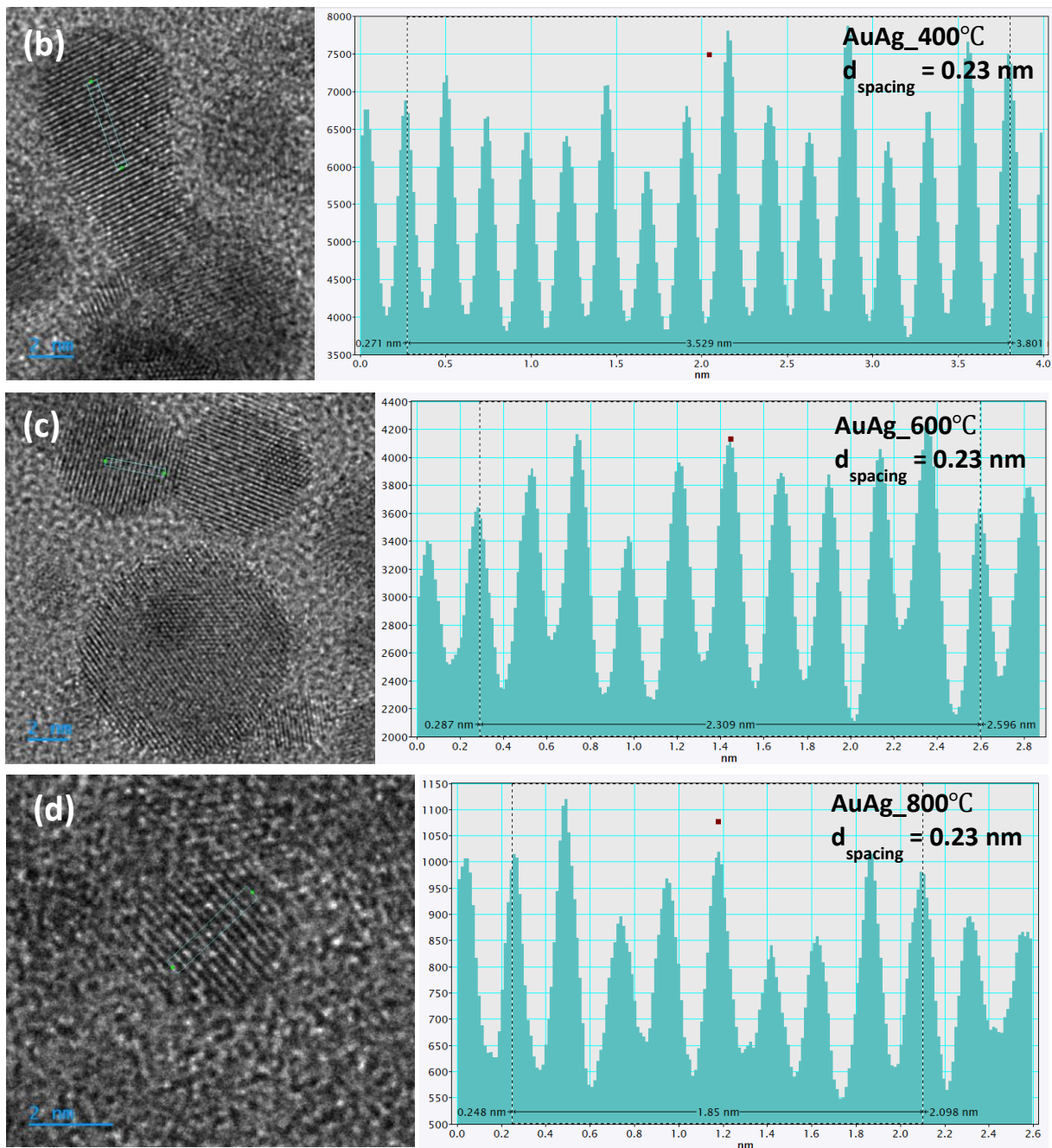


Figure S7. Magnified HRTEM image of AuAg-SiO₂ NC after annealing at different temperatures with well-defined lattice fringes of AuAg NPs (the estimated d_{spacing} and annealing temperature is shown in the image itself). Line profile is also shown alongside. The scale bar of 2 nm is used for all the HRTEM images.

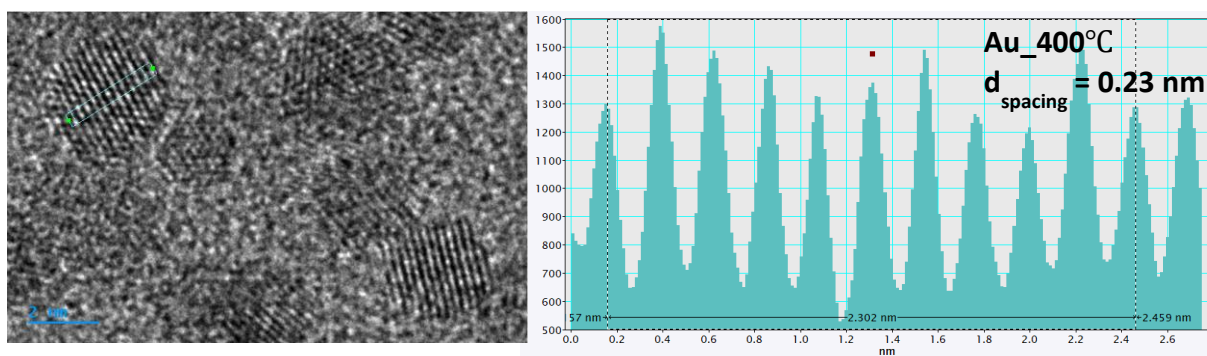


Figure S8. HRTEM image of Au-SiO₂ NC annealed at 400 °C with well-defined lattice fringes. Line scan profile taken over the indicated area to calculate the lattice spacing. The d_{spacing} is estimated as 0.23 nm. The scalebar of 2 nm is used.

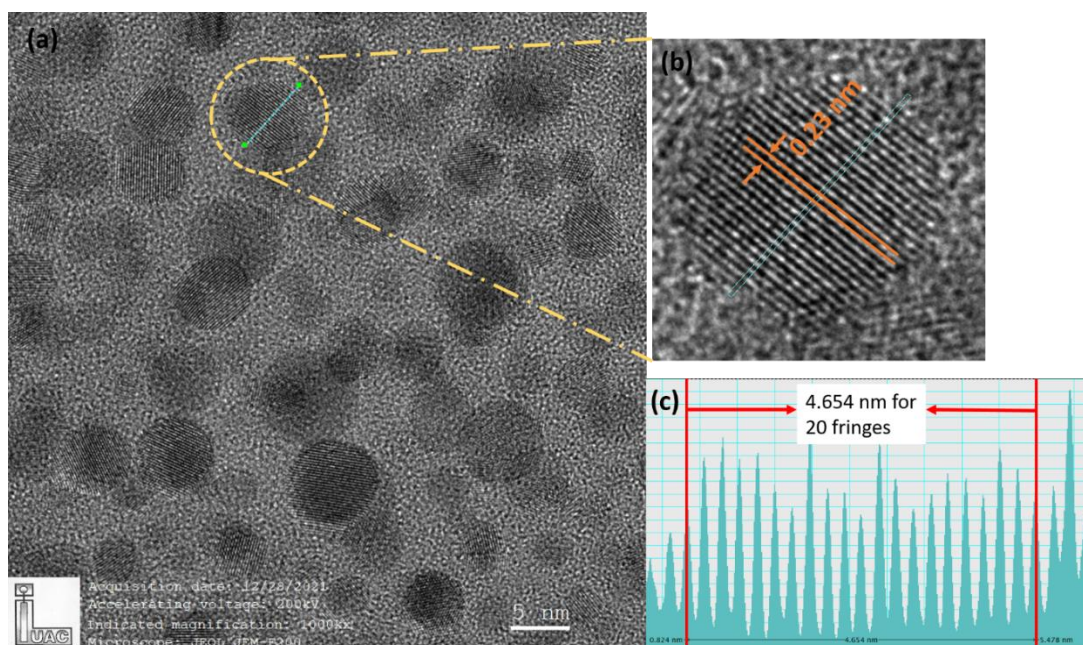


Figure S9. (a) HRTEM images of Ag-SiO₂ NC at 800 °C (b) Enlarge portion of HRTEM image indicating the spacing between two fringes (c) Line scan profile taken over the circled area to calculate the lattice spacing.

X-ray photoelectron spectroscopy (XPS) measurements:

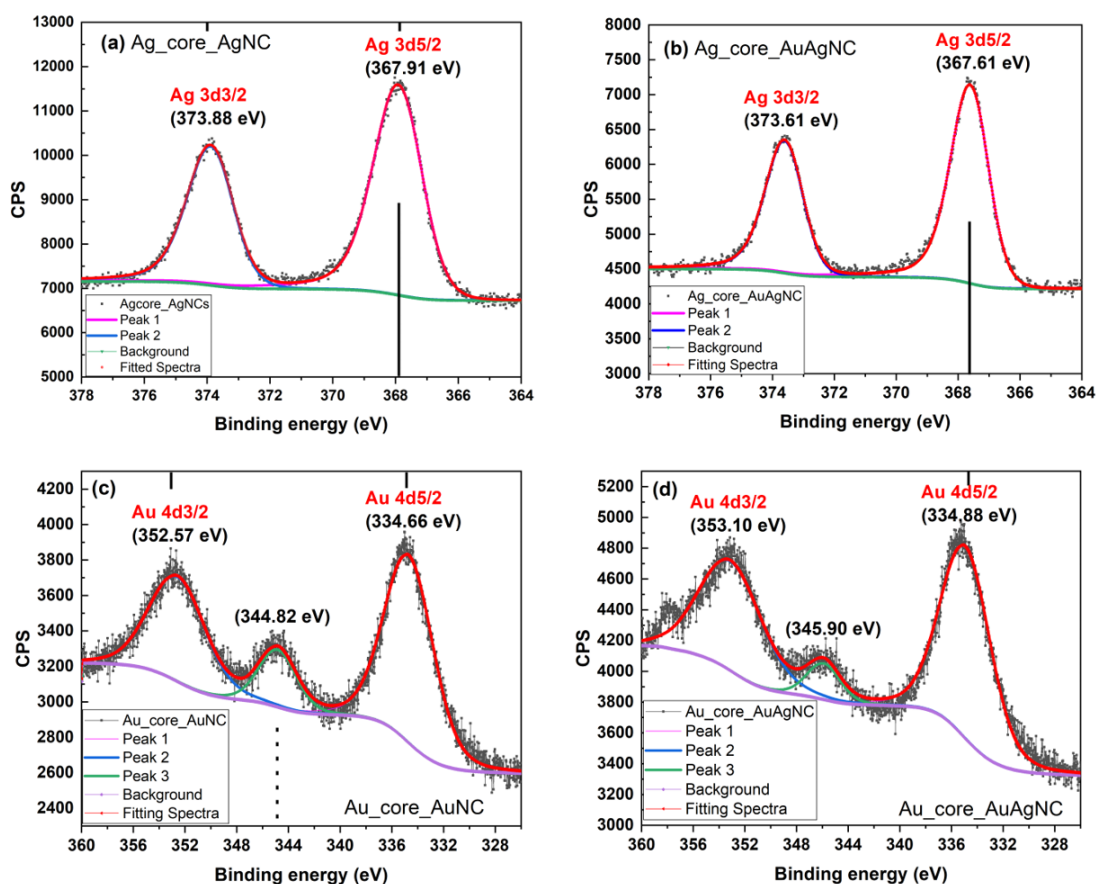


Figure S10. The core-level XPS spectra of the Ag component of the (a) Ag/SiO₂ NC and (b) AuAg/SiO₂ NC are presented. Prior to peak fitting, Shirley background has been subtracted from spectrum as shown with green line (in upper spectra) and magenta lines (in lower spectra). For Ag component, two asymmetric Lorentzian peaks were selected to accurately fit the curve. The fitted spectra is represented by red color. The core-level XPS spectra of the Au component of the (c) Au/SiO₂ NC and (d) AuAg/SiO₂ NC are shown. The background correction is performed using the same procedure as followed for the Ag component. However, unlike Ag component, three peaks are used here to fit the spectra. Asymptotic Doniach Sunjic/Gaussian-Lorentzian line shape is used for Au components.

X-ray photoelectron spectroscopy (XPS) is an effective and sensitive technique for determining changes in the chemical state of any element at the surface (~5-10 nm). The fitted XPS spectrum of Ag/SiO₂ NC are shown in Fig. S10(a). Shirley background correction is used to filter out in-elastically scattered background photoelectrons. To fit the experimental spectra, Lorentzian asymmetric line shape is used. The 3d band of Ag is splitting into two peaks (Ag 3d5/2 and Ag 3d3/2) due to spin-orbital coupling. The Ag 3d5/2 spectra is fitted using a single asymmetric peak, with peak position centred at 367.91 eV (FWHM = 1.77 eV). The Ag 3d3/2 peak, which is centred at 373.88 eV (FWHM = 1.66 eV), is similarly fitted with a single peak. These assigned peaks and their positions are in good agreement with previously reported data [6-8]. For both the peaks of Ag 3d level, the domination of Ag⁰ peak is seen with no additional trailing, confirming the absence of oxidation state of Ag [7]. The pure state of Ag NPs with no oxidation is also confirmed by HRTEM images. Fig. S10(c) shows the XPS spectra of Au component of Au/SiO₂ NC. Here, Lorentzian asymmetric line shape is utilised for both the chosen peaks 1 and peak 2 to match the observed spectra. For the corresponding BE values of

334.66 eV (FWHM = 4.47 eV) and 352.57 eV (FWHM = 5.09 eV), these peaks are identified as Au 4d_{5/2} and Au 4d_{3/2}, respectively. Around 344.82 eV, an extra peak is seen. This additional peak might be a result of the resonance peak, satellite peak, or oxidation peak.

The XPS spectra for Ag3d and Au4d components of AuAg/SiO₂ NC and their respective fitted spectra are shown in Fig S10 (b & d). As per Fig. S 10(b), the peak position for splitted Ag 3d_{5/2} and Ag 3d_{3/2} component is centred at 367.61 eV (FWHM = 1.40 eV) and 373.61 eV (FWHM = 1.39 eV) respectively. Moreover, the peak positions of Au 4d_{5/2} and Au 4d_{3/2} are respectively centred at 334.88 eV (FWHM = 4.54 eV) and 353.10 eV (FWHM = 5.68 eV), as shown in Fig. S 10(d). It is observed that a negative shift of 0.3 eV in the B.E. is observed for Ag 3d component of AuAg/SiO₂ NC with respect to Ag/SiO₂ NC and a positive shift of 0.2 eV is observed for Au 4d component of AuAg/SiO₂ NC with respect to Au/SiO₂ NC. The observed shift in the B.E. is in accordance with the previous literatures, indicating the formation of alloy NPs due to partial charge transfer between two constituent metals [6, 7, 9].

The effect of high-temperature annealing on surrounding silica thin-film (without metal concentration) deposited on quartz:

In nanocomposite system, it is expected that the metal NPs are buried well inside the silica matrix and will have no direct contact with substrate. Therefore the substrate and substrate temperature can only influence the surrounding matrix and associated optical absorption spectra. Thus, UV-Visible spectroscopy was performed on below-mentioned samples and the results are shown in Fig. S11:

- 1) Silica layer deposited on quartz substrate (As-deposited sample).
- 2) Silica layer deposited on quartz substrate annealed at 800 °C.

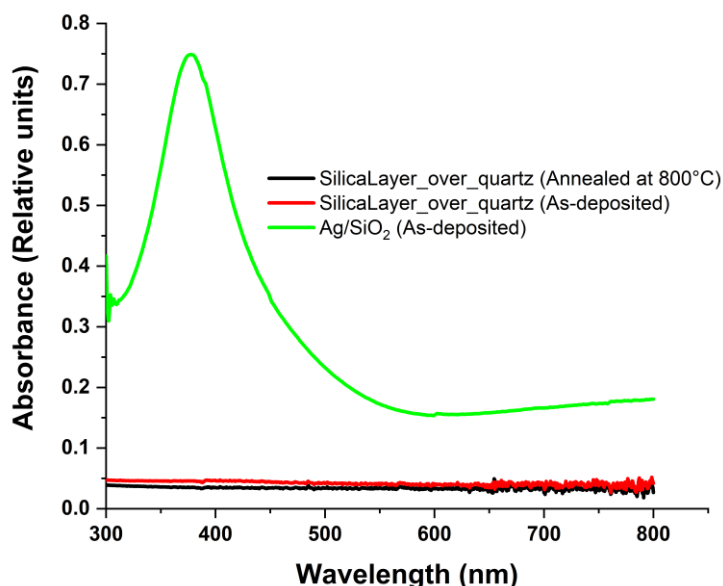


Figure S11. Optical absorbance of as-deposited (red) and 800 °C annealed (black) silica thin-film (without metal) deposited on quartz substrate. The thickness of silica thin film is 260 nm. The absorbance spectra of Ag/SiO₂ nanocomposite (green line) is also included to compare the absorption intensity of silica thin film with and without metal concentration.

It can be seen from Fig. S11 that even after annealing at high temperature (800 °C), the behaviour of the optical spectra remain same and the silica matrix exhibits no optical absorption in the visible region. On the other hand, inclusion of Ag NPs the silica significantly enhances the absorbance due to Ag/SiO₂ LSPR (shown by green line). Therefore, we can conclude that the effect of the substrate annealing on the silica matrix is negligible and that the obtained absorption spectra are primarily because of the embedded metal NPs.

References:

- 1) H. Jatav, M. Shabaninezhad, M. Micetic, A. Chakravorty, A. Mishra, M. Schwartzkopf, A. Chumakov, S. V. Roth and D. Kabiraj, *Langmuir*, 2022, **38**, 11983–11993.
- 2) L. R. Doolittle, *Nucl. Instru. Metho. in Phy. Res. Sec. B: Beam Interac. with Mat. and Atoms*, 1985, **9**, 344–351.
- 3) M. Buljan, N. Radic, S. Bernstorff, G. Dražic, I. Bogdanovic Radovic and V. Holy, *Acta Crystallogr. Sec. A: Foundat. Crystallo.*, 2012, **68**, 124–138.
- 4) L. Basioli, K. Salamon, M. Tkalcevic, I. Mekterovic, S. Bernstorff and M. Micetic, *Crystals*, 2019, **9**, 479.
- 5) P. Pandit, M. Schwartzkopf, A. Rothkirch, S. V. Roth, S. Bernstorff and A. Gupta, *Nanomaterials*, 2019, **9**, 1249.
- 6) R. Watson, J. Hudis and M. Perlman, *Phy. Rev. B*, 1971, **4**, 4139.
- 7) T.W. Liao, A. Yadav, K. J. Hu, J. van der Tol, S. Cosentino, F. D’Acapito, R. E. Palmer, C. Lenardi, R. Ferrando, D. Grandjean *et al.*, *Nanoscale*, 2018, **10**, 6684–6694.
- 8) Bzowski, "Electronic structure of AuAg bimetallics: Surface alloying on Ru (001)." *Physical Review B* 59, no. **20** (1999): 13379.
- 9) Gelatt Jr and H. Ehrenreich, *Phy. Rev. B*, 1974, **10**, 398.